

Shaping Sparse Rewards in Reinforcement Learning: A Semi-supervised Approach

Wenyun Li ^{*1} and Wenjie Huang²

¹*Department of Mathematics, The University of Hong Kong, Hong Kong SAR*

²*Department of Data and Systems Engineering, The University of Hong Kong, Hong Kong SAR*

²*Musketeers Foundation Institute of Data Science, The University of Hong Kong, Hong Kong SAR*

Abstract

In many real-world scenarios, reward signal for agents are exceedingly sparse, making it challenging to learn an effective reward function for reward shaping. To address this issue, our approach performs reward shaping not only by utilizing non-zero-reward transitions but also by employing the *Semi-Supervised Learning* (SSL) technique combined with a novel data augmentation to learn trajectory space representations from the majority of transitions, zero-reward transitions, thereby improving the efficacy of reward shaping. Experimental results in Atari and robotic manipulation demonstrate that our method effectively generalizes reward shaping to sparse reward scenarios, achieving up to four times better performance in reaching higher best scores compared to curiosity-driven methods. The proposed *double entropy data augmentation* enhances performance, showcasing a 15.8% increase in best score over other augmentation methods.

1 Introduction

The sparse reward problem is a core challenge in Reinforcement Learning (RL) when solving real-world tasks Kober u. a. (2013). In supervised learning, supervision signals are provided by the training data. In reinforcement learning, rewards take on the role of supervision signals, guiding the agent to optimize its policy. Many real-world tasks naturally have the feature of delayed or infrequent rewards due to the complexity and nature of the tasks. In tasks like Go Silver u. a. (2016), navigation Wang u. a. (2020), or robotic arm manipulation Gu u. a. (2017); Riedmiller u. a. (2018), agents only receive rewards upon successfully achieving the final goal, such as winning a game, reaching a target, or completing a grasp, with no feedback for intermediate steps. Sparse reward provides little immediate feedback to guide the agent’s exploration and high variance in returns, makes it difficult to learn the optimal policy Plappert u. a. (2018b).

A potential solution to tackle the sparse reward problem is *reward design and learning* Ng und Russell (2000). Methods in this category often operate on the replay buffer, processing off-policy data to implement their respective reward design Schaul u. a. (2015); Andrychowicz u. a. (2017); Peng u. a. (2019). Pathak u. a. (2017) propose the Intrinsic Curiosity Module (ICM) that formulates curiosity as the error in an agent’s ability to predict the consequence of its own actions learned by a self-supervised inverse dynamics model. However, curiosity-driven methods face a significant challenge: curiosity, as an intrinsic reward, is inherently decoupled from the actual objectives and tasks. This may cause agents to overly focus on “new” but meaningless states. Kumar u. a. (2019) propose Reward Conditioned Policy (RCP) that treats non-expert trajectories collected from sub-optimal policies as optimal supervision for matching the reward of a given trajectory. However, methods based on suboptimal policies under supervised learning suffer from poor sample efficiency Peng u. a. (2019), especially when non-zero-reward transitions are extremely rare in sparse reward cases.

Moreover, there exists alternative approaches beyond self-supervised methods that may better address the challenges posed by sparse reward data. Raileanu u. a. (2020) utilize data augmentation to enhance RL algorithm, yet such augmentation methods are restricted to image data and tend to lose or distort information in non-vision-based

*Corresponding author: u3637311@connect.hku.hk

task, as the nature of image data is inherently different from that of time-series data, text data, or feature vector data.

In this paper, our approach performs reward shaping not only by utilizing non-zero-reward transitions but also by employing *Semi-Supervised Learning* (SSL) technique to learn trajectory space representations from the majority of transitions, *i.e.*, zero-reward transitions, thereby improving reward shaping, it could help bridge the gap in handling sparse rewards.

Explicitly, we propose an RL algorithm that applies the idea of SSL, called Semi-Supervised Reward Shaping framework (SSRS), and also propose a new data augmentation technique *double entropy data augmentation* specifically for non-image-based task as part of the RL pipeline. By progressively approximating the state-value function and the action-state function, we shape the reward in sparse-reward trajectories. Consistency regularization to both zero-reward and non-zero-reward transitions is adopted for the optimization of the reward estimator. Additionally, a monotonicity constraint is incorporated over the two components of the reward shaping estimator to further reduce the discrepancy between the shaped reward distribution and the true reward distribution.

We evaluate the performance of SSRS in reward-sparse Atari and robotic manipulation environments, comparing it with ICM Pathak u. a. (2017), RCP Kumar u. a. (2019), Prioritized Experience Replay (PER, Schaul u. a. (2015)). Our model demonstrates performance comparable to ICM in Atari environments and achieves a maximum increase over ICM by a factor of four in reaching higher best scores. We further validate that the proposed *double entropy data augmentation* enhances performance showcasing a 15.8% increase in best score compared to other augmentation methods.

2 Related Work

Currently, research aiming at addressing the sparse reward problem mainly focuses on the following areas: experience replay mechanisms Peng u. a. (2019) and reward design and learning. Schaul u. a. (2015) develop a framework for prioritizing experience, so as to replay important transitions more frequently, and therefore learn more efficiently. Memarian u. a. (2021) leverage self-supervised methods to extract signals from trajectories while simultaneously updating the policy. Andrychowicz u. a. (2017) propose Hindsight Experience Replay (HER) that allows sample-efficient learning from rewards which are sparse and binary and therefore performs well especially on robotic manipulation tasks. Ng und Russell (2000) propose the idea of learning reward functions from optimal interaction sequences, known as Inverse Reinforcement Learning (IRL). Brown u. a. (2019) propose an IRL algorithm that outperforms the demonstrator by extrapolating beyond a set of ranked demonstrations in order to infer high-quality reward functions.

Besides expert trajectories, reward shaping can also be applied based on different evaluation criteria. Count-based methods Choi u. a. (2018); Ostrovski u. a. (2017); Bellemare u. a. (2016) incentivize agents based on the rarity of states, while curiosity-driven exploration methods reward the agent’s exploratory behavior. ICM Pathak u. a. (2017) defines curiosity as the error in the agent’s ability to predict the consequences of its own actions in a visual feature space. This curiosity signal serves as an intrinsic reward, driving the agent to explore.

Kumar u. a. (2019) employ *supervised learning* techniques, viewing non-expert trajectories collected from sub-optimal policies as optimal supervision for matching the reward of the given trajectory. Peng u. a. (2019) simplify the process into regressing target values for a value function, and weighted target actions for the policy.

Another related direction is the application of data augmentation Shorten und Khoshgoftaar (2019) in RL algorithms Kostrikov u. a. (2020). Hansen und Wang (2020) decouple augmentation from policy learning and is found to significantly advance sample efficiency, generalization, and stability in training over vision-based RL methods. Yarats u. a. (2021) use data augmentation to learn directly from pixels and is able to solve complex humanoid locomotion tasks directly from pixel observations. Studies like Lin u. a. (2019) generate feasible trajectories based on symmetries observed in the trajectory space for robot control tasks, thereby constructing an Invariant Transform Experience Replay framework to address the issue of high sample requirements. Raileanu u. a. (2020) explore the use of data augmentation techniques in visual RL tasks, such as random cropping, random noise, and color jittering, to improve the robustness of the policy $\pi(a|s)$ and the value function $V(s)$.

3 Methodology

In this section, we introduce the proposed method by first introducing the proposed *double entropy data augmentation*, followed by the SSRS framework, featuring a monotonicity constraint and *consistency regularization*.

3.1 Double Entropy Data Augmentation

In reinforcement learning, applying invariant transformations to trajectories can improve the generalization performance of both the policy network and the value function network Lin u. a. (2019); Raileanu u. a. (2020). The unitless property of Entropy makes it particularly useful in data augmentation, as it allows for a fair comparison of information content across different features, regardless of their scale or domain. Entropy is essentially a measure of uncertainty or randomness in a probability distribution, and it is calculated in a way that normalizes the result, making it dimensionless. We propose a *double entropy data augmentation* method as follow. *Shannon Entropy* Shannon (1948) quantifies the amount of information required to describe or encode a random variable’s possible states. In RL tasks, observations and trajectories are matrices in practice, but can also be normalized and viewed as discrete random variable. Let X be a discrete random variable with finite sample space \mathcal{X} and probability mass function $p(x) = \Pr\{X = x\}$, $x \in \mathcal{X}$. The entropy $H(X)$ of a discrete random variable X is defined by

$$H(X) := - \sum_{x \in \mathcal{X}} p(x) \log p(x).$$

Consider a $m \times n$ matrix A with each element $a_{ij} \leq 0$, $\forall i = 1, \dots, m, j = 1, \dots, n$, and the *Shannon Entropy* of matrix A is defined by

$$H(A) := - \sum_{k=1}^{mn} p_k \log(p_k), \tag{1}$$

where the probabilities are normalized by the matrix elements as $p_k = a_{ij} / \sum_i \sum_j a_{ij}$, such that $\sum_{k=1}^{mn} p_k = 1$.

Denote state space as $\mathcal{S} \in \mathbb{R}^{m_1}$ and action space as $\mathcal{A} \in \mathbb{R}^{m_2}$, with $m_1, m_2 \geq 1$. Consider a trajectory τ of length N as $\langle s_0, a_0, r_0, s_1, a_1, r_1, \dots, s_N \rangle$ with $a_t \in \mathcal{A}$, $s_t \in \mathcal{S}$, for all $t = 1, \dots, N$, and rewards are given following the environment’s original reward function $r_t = R(s_t, a_t, s'_t)$. The set of all trajectories can be stacked into the matrix $\bar{\Gamma} = [S, A, R]$ with $S \in \mathbb{R}^{N \times m_1}$, $A \in \mathbb{R}^{N \times m_2}$ and $R \in \mathbb{R}^{N \times 1}$, and now we define the transform *double entropy data augmentation* σ over matrix $\bar{\Gamma}$ as:

$$\sigma(\bar{\Gamma}|n) := [[h^1 \cdot s^1, h^2 \cdot s^2, \dots, h^n \cdot s^n], A, R],$$

where $h^n \in \mathbb{R}$, equals to the entropy $H(s^n)$, matrix s^n is a submatrix of the stacked state S , obtained by equally dividing S into n parts along the state dimension. Here n is a hyperparameter and $H(s)$ is the matrix Shannon entropy defined in Eq.(1).

3.2 Semi-Supervised Reward Shaping

The Semi-Supervised Reward Shaping (SSRS) framework proposed in this paper, aims to fit an optimal state-value function $V^*(s)$ and an optimal action-value function $Q^*(s, a)$, which are used to shape the rewards of trajectory Γ . Given an one-step trajectory $\langle s_t, a_t, r_t, s_{t+1} \rangle$, the estimated reward can be calculated from the estimations of the optimal state-value function $V^*(s)$ and the optimal action-value function $Q^*(s, a)$ as follows. We first define the confidence score vector of timestep t over a fixed reward set $Z = \{z_i, i = 1, \dots, N_z\}$ in Eq.(2), where N_z is a hyperparameter controlling the number of estimated rewards. Value of z_i is set according to the collected true reward value, and is updated throughout the process of agent’s interactions with environment.

By the following Eq.(2), we can get confidence vector $\mathbf{q}_t \in \mathbb{R}^{N_z}$ at timestep t , with each $q_i \in \mathbf{q}_t$ corresponding to a estimated reward $z_i \in Z$, computed as

$$\mathbf{q}_t = \beta Q(s_t, a_t) + (1 - \beta)V(s_{t+1}). \tag{2}$$

The reward z estimated from the trajectory $\langle s_t, a_t, r_t, s_{t+1} \rangle$ essentially evaluates the quality of the agent’s interaction with the environment at the current step based on the trajectory. We utilize $Q(s_t, a_t)$ to assess the long-term return (*i.e.*, the cumulative future reward) of taking action a_t in state s_t , and combine this with the future cumulative return estimation $V(s_{t+1})$ of transitioning to state s_{t+1} after taking action a_t in state s_t , which gives us the estimated z in the form of linear combination of the two, with $\beta > 0$. The estimate reward value z_t is selected with maximum confidence score above the threshold λ , *i.e.*, $z_t = \alpha(\mathbf{q}_t, \lambda)$, where

$$\alpha(\mathbf{q}_t, \lambda) = \begin{cases} \arg \max_{z_i} \mathbf{q}_t, & \text{for } q_i > \lambda, i = 1, \dots, N_z, \\ 0, & \text{else.} \end{cases}$$

A Monotonicity Constraint in SSRS

The value function $V(s_t)$ provides a global baseline for a state, while advantage function captures the relative advantage or disadvantage of action a with respect to this baseline. This separation makes it easier to assess the relative importance of specific actions, and thus compensates for the insensitivity to actions because the disturbance of data augmentation only take place on state s . By utilizing the relationship between V and Q , we can introduce the monotonicity constraint in the SSRS framework as follows, which quantifies the mean square positive advantage function values. Define $\delta_t(\theta) = Q(s_t, a_t, \theta_1) - V(s_t, \theta_2)$ where θ is the combination of θ_1 and θ_2 , we have

$$L_{QV} = \begin{cases} 0, & \delta_t(\theta) < 0, \\ \frac{1}{\mu B} \sum_{t=1}^{\mu B} (\delta_t(\theta))^2, & \text{else.} \end{cases} \quad (3)$$

Note that μ represents the proportion of non-zero rewards in the buffer, which quantifies the sparsity level, and B is the batch size of trajectories. Minimizing the objective loss L_{QV} over the parameter θ of can achieve a more stable update, which will be validated in Section 4.3, and is crucial to SSRS framework’s success.

B Consistency Regularization in SSRS

Consistency regularization is an important component of algorithms in the field of SSL Bachman u. a. (2014). The reward estimator, as a crucial component in *reward shaping*, needs to capture the invariance of trajectories, which refers to the reward unaffected by minor variations in input transitions, aligning with the characteristics of consistency regularization. Furthermore, in scenarios with sparse rewards, applying weak strong augmentations to transitions with zero and non-zero reward transitions before conducting consistency regularization further enhances the generalization ability of the reward estimator in sparse reward environments. Note that the vector \mathbf{q}_t , the confidence of the reward predictions under the trajectory $\langle s_t, a_t, r_t, s_{t+1} \rangle$, consists of $Q(s_t, a_t, \theta_1)$ and $V(s_{t+1}, \theta_2)$. To be explicit, we use $\mathbf{q}_t(\theta)$ to show its dependence in θ . In order to obtain the optimal θ value for accurately estimating the reward value of each trajectory $\langle s_t, a_t, r_t, s_{t+1} \rangle$, SSRS framework first optimizes the following objective loss function:

$$L_r = \frac{1}{\mu B} \sum_{t=1}^{\mu B} \mathbb{1}(\max(\mathbf{q}_t(\theta)) \geq \lambda) (r_t - \mathbf{q}_t(\theta))^2. \quad (4)$$

SSRS also computes the loss on sparse reward trajectories as shown in Eq.(5), which is the loss between the strong augmentation term and weak augmentation term. Assuming continuity of trajectories in the metric space, it calculates the confidence of reward values after weak and strong augmentations, denoted by \mathbf{q}_t^w and \mathbf{q}_t^s , respectively. Here we omit their dependence on θ for simplicity. The weak and strong augmentations refer to Table 5 in Appendix, where we consider Gaussian noise with smaller parameters as weak augmentation, and other augmentation such as smoothing, translation, and cutout, with larger parameters as strong augmentation. For confidence values greater than the threshold in weak augmentation, the one-hot operation is performed Bachman u. a. (2014), denoted as $\mathbf{q}_t^{w,'}$, and then used to compute the cross-entropy loss with the normalized confidence values greater than the threshold in strong augmentation, denoted as $\mathbf{q}_t^{s,'}$. The loss function is denoted as.

$$L_s = \frac{1}{(1-\mu)B} \sum_{t=1}^{(1-\mu)B} [\mathbb{1}(\max(\mathbf{q}_t^s) \geq \lambda, \max(\mathbf{q}_t^w) \geq \lambda) \cdot \mathcal{H}(\mathbf{q}_t^{w,'}, \mathbf{q}_t^{s,'})], \quad (5)$$

where \mathcal{H} denotes the cross-entropy, $-\langle \mathbf{q}_t^{w,'}, \log(\mathbf{q}_t^{s,'}) \rangle$. Together, L_r and L_s forms the consistency regularization in the SSRS framework.

C Overall Framework

The illustration of the SSRS framework is shown in Figure 1. We also present the value-based SSRS framework with synchronous update, *i.e.*, *value function update and reward shaping carry out simultaneously.* in Algorithm 1. The loss function of the Semi-Supervised Reward Shaping framework is given by Eq.(3), (4) and (5) above, and

combined by the parameter α . After the agent collects experience, the loss function can be back-propagated either synchronously or asynchronously to initialize the reward estimation network, and the weight of L_s is initialized with a small α . It is important to note that the reward estimation network consists of both the V network and the Q network, and during backpropagation, they are treated as a single entity for gradient computation using the chain rule. In Appendix, we provide the derivations of the “approximate” gradients of loss functions L_{QV} , L_r and L_s with respect to θ , after approximating the indicator functions by sigmoid function.

Algorithm 1 Value-based SSRS Framework (synchronous update)

Require: Confidence threshold λ , loss weight α , set Z with size N_z , episodes T , update probability p_u ;

- 1: Initialize parameters θ , Q function, replay buffer \mathcal{D} ;
- 2: **for** $t = 1$ to T **do**
- 3: **repeat**
- 4: Take a_t from s_t using policy derived from Q (e.g., ϵ -greedy), observe r_t, s_{t+1}
- 5: **if** $r_t \notin \{r_1, \dots, r_{t-1}\}$ **then**
- 6: Obtain N_z new z_i by interpolating from all historical observation r_1, \dots, r_t
- 7: **end if**
- 8: **if** $r_t = 0$ **then**
- 9: Calculate confidence $\mathbf{q}_t(\theta)$ over set Z under parameter θ .
- 10: Perform reward shaping on zero-reward transitions in \mathcal{D} of the p_u ratio.
- 11: **end if**
- 12: Choose a batch of transitions \mathcal{B} from \mathcal{D} . Update Q function with shaped reward \hat{r} ,

$$Q(s, a) \leftarrow Q(s, a) + \alpha \cdot \frac{1}{|\mathcal{B}|} \sum_{(s, a, \hat{r}, s') \in \mathcal{B}} \left(\hat{r} + \gamma \max_a Q(s', a) - Q(s, a) \right).$$

- 13: **until** s_{t+1} is the terminal state
 - 14: Update parameter θ through minimizing the objective $L = L_{QV} + \alpha L_s + (1 - \alpha)L_r$
 - 15: **end for**
-

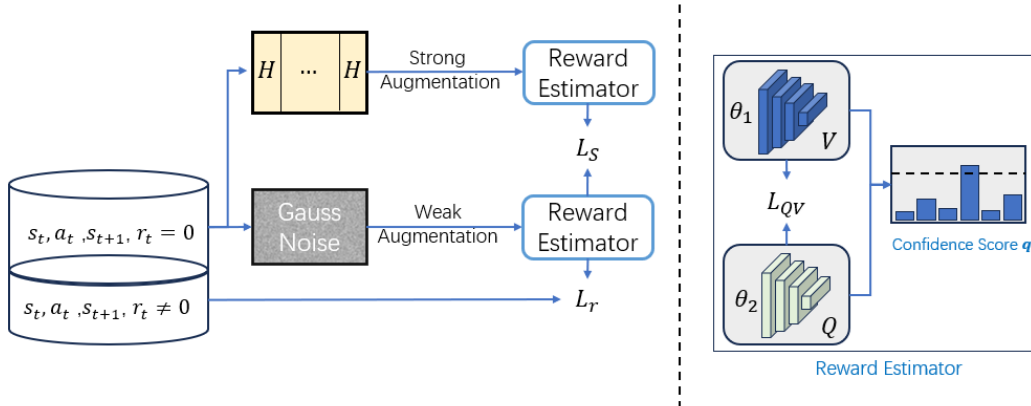


Figure 1: SSRS framework. $r_t = 0$ indicating the sparse reward samples in the buffer and $r_t \neq 0$ indicating samples with non-zero rewards revise the figure a bit.

Before updating the policy gradient or the Q-network parameters in the deep RL algorithm, the reward estimation network is used to sample sparse reward trajectories from the experience replay buffer with probability p_u to compute the estimated reward. In the early stages of training, the update probability p_u is set proportional to $\log(\mu\mathcal{N})$, where $\mu\mathcal{N}$ represents the number of trajectories containing true reward signals. This prevents excessive variance in the initial policy gradient updates or Q-network updates, which is crucial for maintaining stability during the training

process. In the middle stages of training, the update probability p_u is increased to match $\mu\mathcal{N}$, and in the later stages, it is reduced again to be proportional to $\log(\mu\mathcal{N})$, as the model has already learned a good policy and no longer requires a large number of simulated reward signals to assist in descent.

In addition, in the early stages of training, the model relies more on the true rewards from the environment feedback. As training progresses, the model will output reward estimates with increasingly higher confidence, i.e., satisfying $\max(\mathbf{q}_t) \geq \lambda$, while also learning more domain knowledge of the trajectory space with increasing coefficient α .

4 Experiment Results

The experiments aim to validate the performance of the SSRS framework in both the Atari game environment Belle-mare u. a. (2013) and the robotics manipulation environment Plappert u. a. (2018a) (see Figure 2) and, using Random Access Memor (RAM) observations as an example, demonstrate the superiority of *double entropy data augmentation* over other data augmentation methods. Additionally, ablation experiments are conducted to demonstrate the importance of monotonicity constraints in the application of SSL techniques. Distinct from other reward shaping methods, our paper introduces a semi-supervised pipeline to enhance sample efficiency. In Section 4.4, we will analyze the characteristics of the trajectory space through experiments to provide insights into the underlying reasons of such improvement.

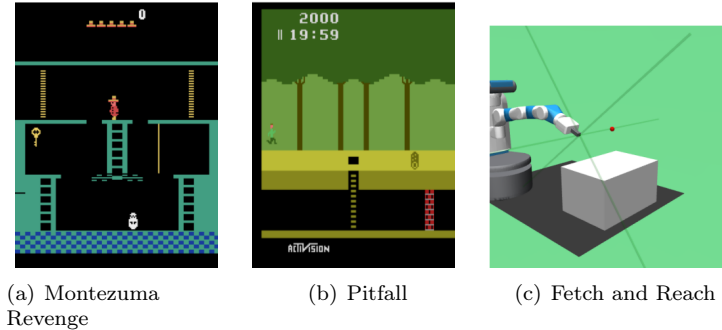


Figure 2: (a) and (b) show the game scenes from Montezuma Revenge and Pitfall in Sparse reward environment of the Arcade Learning Environment (ALE), commonly referred to as Atari. (c) is a snapshot of robotic arm performing Fetch and Reach task in Gymnasium-Robotics environment.

Experimental Setup. RAM observation refers to a representation of the Atari RL environments’ internal state directly from its Random Access Memory, typically 128 bytes of RAM (i.e., a vector of 128 integers, each in the range $[0, 255]$). The code for this experiment is based on the Tianshou RL library Weng u. a. (2022). At each epoch, 2000 transition samples are collected (i.e., 2000 timesteps are executed in the environment) and appended to the dataset \mathcal{D} , a buffer with a capacity of 30k transitions. Some of the hyperparameter settings are as Table 3 in Appendix, which are determined based on preliminary hyperparameter tuning results, and consistent hyperparameter settings are used in both the Robotics and Atari experiments.

4.1 Performance of SSRS

To evaluate the proposed SSRS framework, we compare it with several baselines and benchmarks algorithms in both the Atari and Robotic environments:

- **Intrinsic Curiosity Module (ICM, Pathak u. a. (2017)):** ICM encourages exploration by rewarding the agent for discovering novel states based on intrinsic motivation.
- **Reward Conditioned Policy (RCP, Kumar u. a. (2019)):** RCP conditions views non-expert trajectories collected from suboptimal policies as optimal supervision so as to shape the reward of the given trajectory.
- **Prioritized Experience Replay (PER, Schaul u. a. (2015)):** PER improves learning efficiency by prioritizing experience samples with high temporal difference errors.

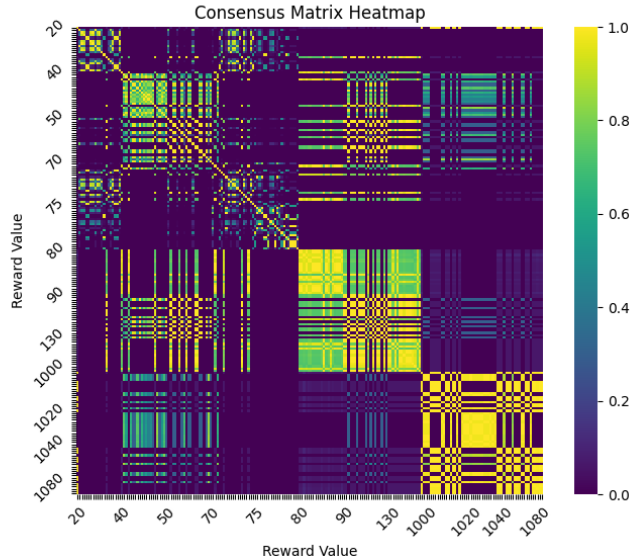


Figure 3: this consensus matrix of reward distribution in Hero-ram-v4 after 1000 episodes iterations indicates that the distribution of trajectories along the reward dimension in the regulatory space exhibits a certain clustering property. The cluster method used is Gauss Mixture Models, and the number of iterations for consensus matrix is 100.

The baseline algorithms for both Atari and Robotic environments are Deep Q-Network (DQN, Mnih u. a. (2015)) and Deep Deterministic Policy Gradient (DDPG, Lillicrap u. a. (2015)), respectively. Several variants of the SSRS framework are employed, including SSRS-S, which uses *double entropy augmentation*, SSRS-C, which adopts the cutout method for data augmentation, and SSRS-M, which adopts the smooth method for data augmentation.

In the FetchReach environment in Robotics, where the reward signal is binary, *i.e.*, the reward is -1 if the end effector hasn't reached its final target position, and 0 if the end effector is in the final target position, the SSRS framework outperforms both PER and DDPG (see Figure 4), with the latter two algorithms struggling to learn a successful policy. However, the ICM algorithm performs better than SSRS in this environment by more effectively shaping the reward, achieving a higher best reward. In another sparse while more diverse environment, *i.e.*, Atari (see Figure 5), the SSRS algorithm and its variants outperform the baseline algorithm across all four games. In games with moderate reward sparsity, such as Seaquest and Hero, SSRS achieves performance comparable to the ICM algorithm. In terms of convergence speed, the SSRS-S variants outperform ICM in the Seaquest environment. Moreover, in games with extremely sparse rewards, such as MonteZumaRevenge and Venture, SSRS significantly outperforms the ICM algorithm, achieving nearly 4 times the best score in MonteZumaRevenge (see Figure 5(c)). Evidently, the sparser the rewards in the environment, the more unstably the policy updates, as indicated by the larger variance in the best reward curves. In contrast, SSRS and its variants exhibit superior update stability in Venture during later stages, as shown in Figure 5(d).

4.2 Performance of Data Augmentation

The performance analysis of *double entropy data augmentation* is conducted in Atari environment (see Figure 6). In the first two games, Seaquest and Hero, *double entropy data augmentation* consistently maintains a leading position in terms of both convergence speed and final highest rewards, with the variance of the best reward remaining within a narrow range. In the more reward-sparse environment of MonteZumaRevenge, although the final best reward achieved by the translate augmentation (blue curve) method is higher, it exhibits significantly larger variance. In contrast, *double entropy data augmentation* (green curve) demonstrates much smaller variance (see Figure 6(c)), indicating a more stable policy and a faster update rate. As we will mention in Section 4.4, *double entropy data augmentation* preserves the smoothness and clustering of trajectories better in the trajectory space. This is crucial

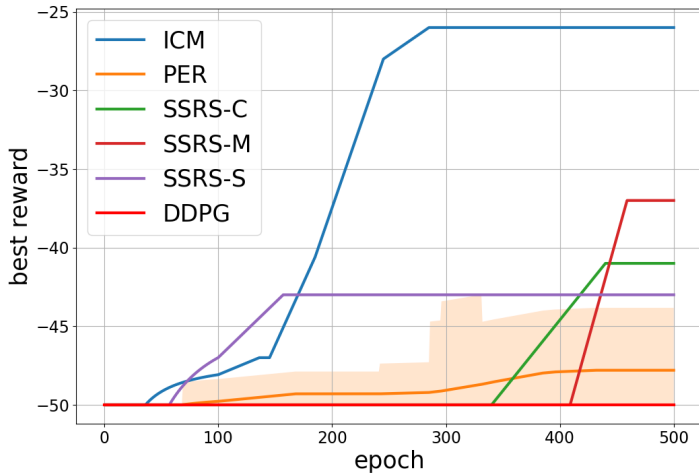


Figure 4: The best score curve of SSRS variants and aforementioned baselines over 500 epochs in the robotic manipulation environment FetchReach.

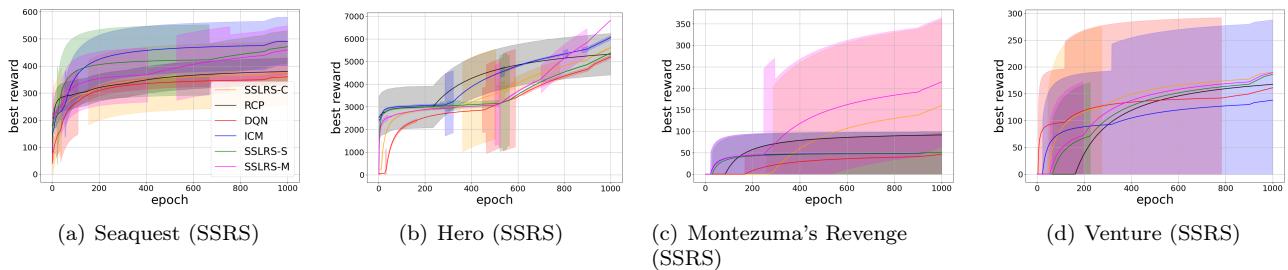


Figure 5: Figures (a–d) demonstrate the best score in 1000 epochs of different algorithms in 4 Atari environments. Different curves represent the SSRS framework and its variants, as well as ICM, RCP and DQN algorithms. The legends of each sub figure are uniformly labeled in Figure(a)

to the step of calculating estimated reward, where the V network and Q network are not able to separate trajectories to learn a good representation of the space. From the perspective of the teacher-student model, such a ‘muddled’ teacher would lead the student, *i.e.* policy module, to learn an unstable policy.

In Venture, *double entropy data augmentation* maintains stable variance throughout (see Figure 6(d)), whereas other data augmentation methods struggle to avoid larger variance in such a sparse environment, where disturbance to the data exceeded the decision-making boundaries of the trajectory space. Moreover, *double entropy data augmentation* achieves a best score that was 10 percentage points higher than the best result among tested image-based data augmentation methods in this environment.

4.3 Ablation Experiments of Monotonicity Constraint

We conduct a series of experiments on the SSRS framework under conditions with and without monotonicity constraint and study the distribution of reward values at different stages of training in both scenarios.

The average best score obtained is presented in Table 1. In all the three environments, SSRS with a monotonicity constraint achieves higher best scores compared to SSRS without a monotonicity constraint. Considering the results from previous two sections, as SSRS-S set (green curves) only differs in monotonicity constraints between SSRS experiments (see Figures 5) and DA experiments (see Figures 6), we find that adding the monotonicity constraint reduces the variance as well as the final best score in reward-sparse environments with long-term goals (see Figure

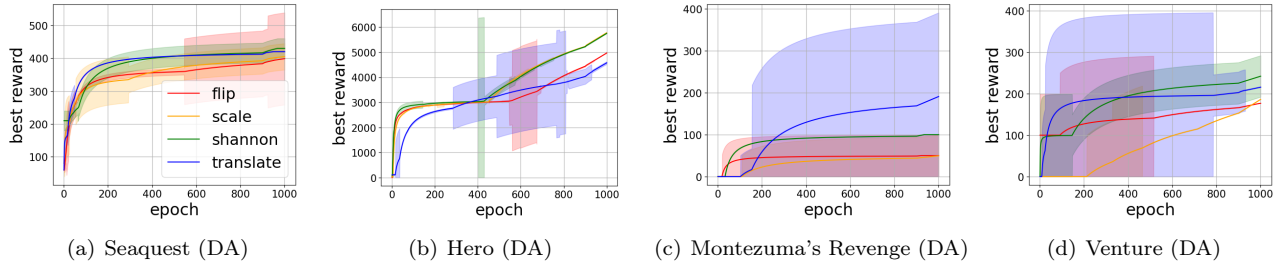


Figure 6: Figures (a–d) demonstrate the best score in 1000 epochs of different data augmentation methods in 4 Atari environments. Note that Shannon refers to *double entropy data augmentation*. The legends of each sub figure are uniformly labeled in Figure(a)

Table 1: Average best score of SSRS framework with monotonicity (SSRS-ST) constraint and without monotonicity constraint (SSRS-NST) in 4 environments.

AVG BEST SCORE	SSRS-ST	SSLRL-NST
SEAQUEST	480	447.5
HERO	8870	7599.5
MONTEZUMA	166.3	100
VENTURE	200	275

5(d) and 6(d)). However in the less reward-sparse Seaquest environment, this constraint increases the variance and the final best score (see Figure 5(a) and 6(a)). The lower variance means a more stable update in policy, but may also reflect an insufficient exploration, resulting in a lower best score compared to the unconstrained case, as observed in Table 1 for the Venture environment. One of the reasons of such difference in sparse and less-sparse scenarios is our strategy of configure in update probability p_u . The hyperparameter p_u is set proportional to the number of non-zero-reward transitions, $\mu\mathcal{N}$. However, the variation in the number of non-zero-reward transitions across different environments is not linear. Although we improved the method by setting p_u to the order of $\log(\mu\mathcal{N})$ during the early stages of training, this adjustment does not cover all possible scenarios.

Further investigation of the reward distribution in Hero (see Figure 7) reveals that, according to the reward distribution of the baseline algorithm without reward shaping, most of the reward signals in this environment consist of small reward values, with a lack of medium to long-term reward feedback. SSRS without a monotonicity constraint only provides reward estimates close to the mean. This may be related to the observation in Section 4.4 that reward values near the mean exhibit better clustering properties. However, this completely deviates from the actual reward distribution of the environment, causing the reward estimator to degrade into a binary classifier. Experimental results also indicate a performance drop without the constraint. In contrast, SSRS with a monotonicity constraint shapes a reward distribution that closely approximates the true reward distribution while also exhibiting the properties of a positively skewed normal distribution.

4.4 Feasibility of Semi-Supervised Learning

SSL methods relies on the smoothness assumption and clustering assumption Ouali u. a. (2020) on the augmented data, in this case, the trajectories. To be specific, the smoothness assumption indicates if two points x_1, x_2 reside in a high-density region are close, then so should be their corresponding outputs y_1, y_2 . And clustering assumption indicates that samples from the same class are closer to each other, while there are significant boundaries between samples from different classes and the decision boundary of the model should be as far as possible from regions of high data density. We examine the trajectory distribution and obtain the consensus matrix \mathcal{C} in Figure 3. Each element $a_{ij} \in \mathcal{C}, 0 \leq a_{ij} \leq 1$, is frequency at which the two trajectories τ_i and τ_j are assigned to the same shaped reward value. Note that we use reward shaped values for labels.

Larger reward values, i.e., rewards given for achieving long-term goals, exhibit clear decision boundaries with smaller reward values. However, the decision boundaries inside high reward values are more ambiguous, with only

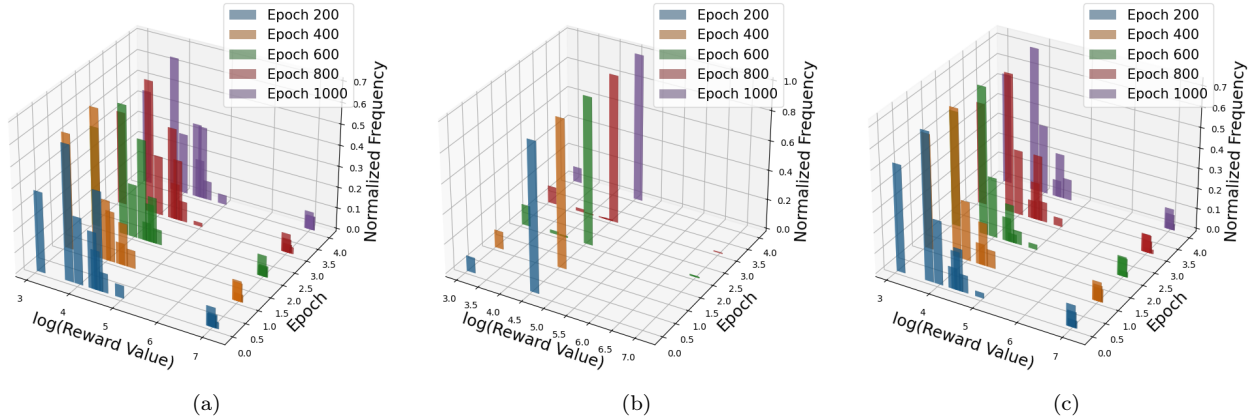


Figure 7: (a) represents SSRS with a monotonicity constraint, (b) represents SSRS without a monotonicity constraint, and (c) represents the baseline algorithm DQN. Shaped rewards from the buffer \mathcal{D} were sampled at epochs 200, 400, 600, 800, and 1000. Since the reward value distribution is sparse, the logarithm of the reward values is used as the x-axis, the y-axis represents values of epoch scale to 1/200, and the z-axis represents the normalized reward distribution probability.

one clear diagonal block, aligning with the clustering assumption. But this ambiguity has minimal impact on SSRS, as the the probabilities of reward estimator output these rewards with high confidence is negligible. By also referring to Figure 7, it can be observed that the three ‘phases’ of significance in the consensus matrix plot correspond to the downward trend of the reward distribution probability in Figure 7. This can be understood from the perspective that as the reward value increases, the randomness of the trajectory decreases, leading to greater clustering significance in the trajectory space, and *vice versa*.

5 Conclusion

In this paper, we propose the Semi-Supervised Reward Shaping (SSRS) framework which utilizes zero reward trajectories by employing SSL technique. Additionally, we introduce the *double entropy data augmentation* method for consistency regularization and apply a monotonicity constraint over modules of reward estimator. Our model outperforms RCP and achieves performance comparable to ICM in Atari environments, with a maximum of fourfold increase in reaching higher best scores. Moreover, the double entropy data augmentation enhances performance showcasing a 15.8% increase in best score compared to other augmentation methods. With SSL techniques, we can deploy agents on significantly sparser trajectory data. From a reverse perspective, it is possible to obtain learnable trajectories by artificially annotating rewards for a minimal number of transitions within a large set of trajectory data.

However, it’s important to note that SSRS also introduces several hyperparameters, such as the update probability of trajectories in the experience replay buffer p_u , which has a significant impact on algorithm performance. The tuning of p_u reflects the balance between exploration and exploitation in this class of reward shaping algorithms. Similar issues were also highlighted in Peng u. a. (2019); Kumar u. a. (2019), where the problem of controlling the reward shaping ratio arises when the reward shaping estimator is suboptimal. Like our paper, the balance shifts towards deciding whether the agent should exploit the reward from the estimator or prioritize exploration. We believe that a theoretical analysis of the dynamic relationship between the optimality of the estimator and the exploration-exploitation ratio would be a valuable direction for future work.

References

[Andrychowicz u. a. 2017] ANDRYCHOWICZ, Marcin ; WOLSKI, Filip ; RAY, Alex ; SCHNEIDER, Jonas ; FONG, Rachel ; WELINDER, Peter ; MCGREW, Bob ; TOBIN, Josh ; PIETER ABBEEL, OpenAI ; ZAREMBA, Wojciech:

- Hindsight experience replay. In: *Advances in neural information processing systems* 30 (2017)
- [Bachman u. a. 2014] BACHMAN, Philip ; ALSHARIF, Ouais ; PRECUP, Doina: Learning with Pseudo-Ensembles. In: *ArXiv abs/1412.4864* (2014). – URL <https://api.semanticscholar.org/CorpusID:8307266>
- [Bellemare u. a. 2013] BELLEMARE, M. G. ; NADDAF, Y. ; VENESS, J. ; BOWLING, M.: The Arcade Learning Environment: An Evaluation Platform for General Agents. In: *Journal of Artificial Intelligence Research* 47 (2013), S. 253–279
- [Bellemare u. a. 2016] BELLEMARE, Marc G. ; SRINIVASAN, Sriram ; OSTROVSKI, Georg ; SCHAUL, Tom ; SAXTON, David ; MUNOS, Rémi: Unifying Count-Based Exploration and Intrinsic Motivation. In: *Neural Information Processing Systems*, URL <https://api.semanticscholar.org/CorpusID:8310565>, 2016
- [Bricken 2021] BRICKEN, Trenton: *RewardConditionedUDRL*. 2021. – URL <https://github.com/TrentBrick/RewardConditionedUDRL>. – Accessed: 2025-01-25
- [Brown u. a. 2019] BROWN, Daniel S. ; GOO, Wonjoon ; NAGARAJAN, Prabhat ; NIEKUM, Scott: Extrapolating Beyond Suboptimal Demonstrations via Inverse Reinforcement Learning from Observations. In: *International Conference on Machine Learning*, URL <https://api.semanticscholar.org/CorpusID:119111734>, 2019
- [Choi u. a. 2018] CHOI, Jongwook ; GUO, Yijie ; MOCZULSKI, Marcin ; OH, Junhyuk ; WU, Neal ; NOROUZI, Mohammad ; LEE, Honglak: Contingency-Aware Exploration in Reinforcement Learning. In: *ArXiv abs/1811.01483* (2018). – URL <https://api.semanticscholar.org/CorpusID:53215593>
- [Gu u. a. 2017] GU, Shixiang ; HOLLY, Ethan ; LILICRAP, Timothy ; LEVINE, Sergey: Deep reinforcement learning for robotic manipulation with asynchronous off-policy updates. In: *2017 IEEE international conference on robotics and automation (ICRA)* IEEE (Veranst.), 2017, S. 3389–3396
- [Hansen und Wang 2020] HANSEN, Nicklas ; WANG, Xiaolong: Generalization in Reinforcement Learning by Soft Data Augmentation. In: *2021 IEEE International Conference on Robotics and Automation (ICRA)* (2020), S. 13611–13617. – URL <https://api.semanticscholar.org/CorpusID:227209033>
- [Kober u. a. 2013] KOBER, Jens ; BAGNELL, J. A. ; PETERS, Jan: Reinforcement learning in robotics: A survey. In: *The International Journal of Robotics Research* 32 (2013), S. 1238 – 1274. – URL <https://api.semanticscholar.org/CorpusID:1932843>
- [Kostrikov u. a. 2020] KOSTRIKOV, Ilya ; YARATS, Denis ; FERGUS, Rob: Image Augmentation Is All You Need: Regularizing Deep Reinforcement Learning from Pixels. In: *ArXiv abs/2004.13649* (2020). – URL <https://api.semanticscholar.org/CorpusID:216562627>
- [Kumar u. a. 2019] KUMAR, Aviral ; PENG, Xue B. ; LEVINE, Sergey: Reward-Conditioned Policies. In: *ArXiv abs/1912.13465* (2019). – URL <https://api.semanticscholar.org/CorpusID:209515630>
- [Lillicrap u. a. 2015] LILICRAP, Timothy P. ; HUNT, Jonathan J. ; PRITZEL, Alexander ; HEES, Nicolas Manfred O. ; EREZ, Tom ; TASSA, Yuval ; SILVER, David ; WIERSTRA, Daan: Continuous control with deep reinforcement learning. In: *CoRR abs/1509.02971* (2015). – URL <https://api.semanticscholar.org/CorpusID:16326763>
- [Lin u. a. 2019] LIN, Yijiong ; HUANG, Jiancong ; ZIMMER, Matthieu ; GUAN, Yisheng ; ROJAS, Juan ; WENG, Paul: Invariant Transform Experience Replay: Data Augmentation for Deep Reinforcement Learning. In: *IEEE Robotics and Automation Letters* 5 (2019), S. 6615–6622. – URL <https://api.semanticscholar.org/CorpusID:220363952>
- [Memarian u. a. 2021] MEMARIAN, Farzaneh ; GOO, Wonjoon ; LIOUTIKOV, Rudolf ; TOPCU, Ufuk ; NIEKUM, Scott: Self-Supervised Online Reward Shaping in Sparse-Reward Environments. In: *2021 IEEE/RSJ International Conference on Intelligent Robots and Systems (IROS)* (2021), S. 2369–2375. – URL <https://api.semanticscholar.org/CorpusID:232147062>

- [Mnih u. a. 2015] MNIH, Volodymyr ; KAVUKCUOGLU, Koray ; SILVER, David ; RUSU, Andrei A. ; VENESS, Joel ; BELLEMARE, Marc G. ; GRAVES, Alex ; RIEDMILLER, Martin A. ; FIDJELAND, Andreas K. ; OSTROVSKI, Georg ; PETERSEN, Stig ; BEATTIE, Charlie ; SADIK, Amir ; ANTONOGLU, Ioannis ; KING, Helen ; KUMARAN, Dharshan ; WIERSTRA, Daan ; LEGG, Shane ; HASSABIS, Demis: Human-level control through deep reinforcement learning. In: *Nature* 518 (2015), S. 529–533. – URL <https://api.semanticscholar.org/CorpusID:205242740>
- [Ng und Russell 2000] NG, Andrew Y. ; RUSSELL, Stuart: Algorithms for Inverse Reinforcement Learning. In: *International Conference on Machine Learning*, URL <https://api.semanticscholar.org/CorpusID:266239314>, 2000
- [Ostrovski u. a. 2017] OSTROVSKI, Georg ; BELLEMARE, Marc G. ; OORD, Aäron van den ; MUNOS, Rémi: Count-Based Exploration with Neural Density Models. In: *ArXiv* abs/1703.01310 (2017). – URL <https://api.semanticscholar.org/CorpusID:2924063>
- [Ouali u. a. 2020] OUALI, Yassine ; HUDELLOT, Céline ; TAMI, Myriam: An Overview of Deep Semi-Supervised Learning. In: *ArXiv* abs/2006.05278 (2020). – URL <https://api.semanticscholar.org/CorpusID:219558952>
- [Pathak u. a. 2017] PATHAK, Deepak ; AGRAWAL, Pulkit ; EFROS, Alexei A. ; DARRELL, Trevor: Curiosity-Driven Exploration by Self-Supervised Prediction. In: *2017 IEEE Conference on Computer Vision and Pattern Recognition Workshops (CVPRW)* (2017), S. 488–489. – URL <https://api.semanticscholar.org/CorpusID:20045336>
- [Peng u. a. 2019] PENG, Xue B. ; KUMAR, Aviral ; ZHANG, Grace ; LEVINE, Sergey: Advantage-Weighted Regression: Simple and Scalable Off-Policy Reinforcement Learning. In: *ArXiv* abs/1910.00177 (2019). – URL <https://api.semanticscholar.org/CorpusID:203610423>
- [Plappert u. a. 2018a] PLAPPERT, Matthias ; ANDRYCHOWICZ, Marcin ; RAY, Alex ; MCGREW, Bob ; BAKER, Bowen ; POWELL, Glenn ; SCHNEIDER, Jonas ; TOBIN, Josh ; CHOCIEJ, Maciek ; WELINDER, Peter ; KUMAR, Vikash ; ZAREMBA, Wojciech: *Multi-Goal Reinforcement Learning: Challenging Robotics Environments and Request for Research*. 2018
- [Plappert u. a. 2018b] PLAPPERT, Matthias ; ANDRYCHOWICZ, Marcin ; RAY, Alex ; MCGREW, Bob ; BAKER, Bowen ; POWELL, Glenn ; SCHNEIDER, Jonas ; TOBIN, Joshua ; CHOCIEJ, Maciek ; WELINDER, Peter ; KUMAR, Vikash ; ZAREMBA, Wojciech: Multi-Goal Reinforcement Learning: Challenging Robotics Environments and Request for Research. In: *ArXiv* abs/1802.09464 (2018). – URL <https://api.semanticscholar.org/CorpusID:3619030>
- [Raileanu u. a. 2020] RAILEANU, Roberta ; GOLDSTEIN, Maxwell ; YARATS, Denis ; KOSTRIKOV, Ilya ; FERGUS, Rob: Automatic Data Augmentation for Generalization in Deep Reinforcement Learning. In: *ArXiv* abs/2006.12862 (2020). – URL <https://api.semanticscholar.org/CorpusID:219980275>
- [Riedmiller u. a. 2018] RIEDMILLER, Martin A. ; HAFNER, Roland ; LAMPE, Thomas ; NEUNERT, Michael ; DEGRAVE, Jonas ; WIELE, Tom V. de ; MNIH, Volodymyr ; HEES, Nicolas Manfred O. ; SPRINGENBERG, Jost T.: Learning by Playing - Solving Sparse Reward Tasks from Scratch. In: *International Conference on Machine Learning*, URL <https://api.semanticscholar.org/CorpusID:3562704>, 2018
- [Schaul u. a. 2015] SCHAUL, Tom ; QUAN, John ; ANTONOGLU, Ioannis ; SILVER, David: Prioritized Experience Replay. In: *CoRR* abs/1511.05952 (2015). – URL <https://api.semanticscholar.org/CorpusID:13022595>
- [Shannon 1948] SHANNON, Claude E.: A mathematical theory of communication. In: *Bell Syst. Tech. J.* 27 (1948), S. 623–656. – URL <https://api.semanticscholar.org/CorpusID:55379485>
- [Shorten und Khoshgoftaar 2019] SHORTEN, Connor ; KHOSHGOFTAAR, Taghi M.: A survey on Image Data Augmentation for Deep Learning. In: *Journal of Big Data* 6 (2019), S. 1–48. – URL <https://api.semanticscholar.org/CorpusID:195811894>
- [Silver u. a. 2016] SILVER, David ; HUANG, Aja ; MADDISON, Chris J. ; GUEZ, Arthur ; SIFRE, L. ; DRIESSCHE, George van den ; SCHRITTWIESER, Julian ; ANTONOGLU, Ioannis ; PANNEERSHELVAM, Vedavyas ; LANCTOT,

- Marc ; DIELEMAN, Sander ; GREWE, Dominik ; NHAM, John ; KALCHBRENNER, Nal ; SUTSKEVER, Ilya ; LILICRAP, Timothy P. ; LEACH, Madeleine ; KAVUKCUOGLU, Koray ; GRAEPEL, Thore ; HASSABIS, Demis: Mastering the game of Go with deep neural networks and tree search. In: *Nature* 529 (2016), S. 484–489. – URL <https://api.semanticscholar.org/CorpusID:515925>
- [Wang u. a. 2020] WANG, Chao ; WANG, Jian ; WANG, Jingjing ; ZHANG, Xudong: Deep-Reinforcement-Learning-Based Autonomous UAV Navigation With Sparse Rewards. In: *IEEE Internet of Things Journal* 7 (2020), S. 6180–6190. – URL <https://api.semanticscholar.org/CorpusID:213247194>
- [Weng u. a. 2022] WENG, Jiayi ; CHEN, Huayu ; YAN, Dong ; YOU, Kaichao ; DUBURCQ, Alexis ; ZHANG, Minghao ; SU, Yi ; SU, Hang ; ZHU, Jun: Tianshou: A Highly Modularized Deep Reinforcement Learning Library. In: *Journal of Machine Learning Research* 23 (2022), Nr. 267, S. 1–6. – URL <http://jmlr.org/papers/v23/21-1127.html>
- [Yarats u. a. 2021] YARATS, Denis ; FERGUS, Rob ; LAZARIC, Alessandro ; PINTO, Lerrel: Mastering Visual Continuous Control: Improved Data-Augmented Reinforcement Learning. In: *ArXiv* abs/2107.09645 (2021). – URL <https://api.semanticscholar.org/CorpusID:236134152>

A The Gradients of Loss Functions

A.1 The Gradient of L_{QV}

For L_{QV} mentioned in Section 3.2 in the following explicit form:

$$L_{QV} = \begin{cases} 0, & Q(s_t, a_t, \theta_1) - V(s_t, \theta_2) < 0, \\ \frac{1}{\mu B} \sum_{t=1}^{\mu B} (Q(s_t, a_t, \theta_1) - V(s_t, \theta_2))^2, & \text{else.} \end{cases}$$

Denote $\delta_t(\theta) = Q(s_t, a_t, \theta_1) - V(s_t, \theta_2)$. Consider a batch of size B , within which a proportion $\mu \geq 0$ of the samples satisfy $\delta_t(\theta) < 0$. The remaining proportion $(1 - \mu)$ contributes to the gradient with respect to the parameter $\theta = (\theta_1, \theta_2)$ is given by:

$$\frac{\partial L_{QV}}{\partial \theta} = \frac{2}{(1 - \mu)B} \sum_{t \in \mathcal{I}_+} Q(s_t, a_t, \theta_1) - V(s_t, \theta_2) \cdot \begin{bmatrix} \nabla_{\theta_1} Q(s_t, a_t, \theta_1) \\ -\nabla_{\theta_2} V(s_t, \theta_2) \end{bmatrix}.$$

Here, \mathcal{I}_+ denotes the set of indices for which $Q(s_t, a_t, \theta_1) - V(s_t, \theta_2) \geq 0$.

A.2 The Gradient of L_r

Consider loss function L_r in Eq.(4) as follow

$$L_r = \frac{1}{\mu B} \sum_{t=1}^{\mu B} \mathbb{1}(\max(\mathbf{q}_t) \geq \lambda) (r_t - \alpha(\mathbf{q}_t, \lambda))^2,$$

where confidence score $\mathbf{q}_t = \beta Q(s_t, a_t, \theta_1) + (1 - \beta)V(s_{t+1}, \theta_2)$. Note that the indicator function $\mathbb{1}(\max(\mathbf{q}_t) \geq \lambda)$ is not differentiable due to its discontinuity at the boundary of $\max(\mathbf{q}_t) \geq \lambda$. The derivative of the indicator function only has non-zero contribution at the boundary, *i.e.* $\max(\mathbf{q}_t) = \lambda$. In order to derive the gradient of L_r , we approximate the indicator function $\mathbb{1}(\max(\mathbf{q}_t) \geq \lambda)$ using differentiable function, for simplicity, the sigmoid function, achieving the effect of approximate binary selection:

$$\mathbb{1}(\max(\mathbf{q}_t) \geq \lambda) \approx \sigma(\max(\mathbf{q}_t) - \lambda),$$

where the sigmoid function $\sigma(x)$ is defined as:

$$\sigma(x) = \frac{1}{1 + \exp(-x)}. \quad (6)$$

Thus, the loss function becomes:

$$L_r = \frac{1}{\mu B} \sum_{t=1}^{\mu B} \sigma(\max(\mathbf{q}_t) - \lambda) (r_t - \alpha(\mathbf{q}_t, \lambda))^2.$$

We want to compute the gradient of L_r with respect to $\theta = (\theta_1, \theta_2)$. The loss function has two parts that depend on θ_1 and θ_2 : one is \mathbf{q}_t , and the other is $\alpha(\mathbf{q}_t, \lambda)$. The gradients of the former are:

$$\begin{aligned} \frac{\partial \mathbf{q}_t}{\partial \theta_1} &= \beta \frac{\partial Q(s_t, a_t, \theta_1)}{\partial \theta_1}, \\ \frac{\partial \mathbf{q}_t}{\partial \theta_2} &= (1 - \beta) \frac{\partial V(s_{t+1}, \theta_2)}{\partial \theta_2}, \end{aligned} \quad (7)$$

Thus, the loss function L_r can be rewritten as:

$$L_r = \frac{1}{\mu B} \sum_{t=1}^{\mu B} f_r e_t^2,$$

where f_r is the sigmoid function $\sigma(\max(\mathbf{q}_t) - \lambda)$ defined in Eq.(6) and $e_t = r_t - \alpha(\mathbf{q}_t, \lambda)$. The derivative of f_r with respect to θ_1 is:

$$\frac{\partial f_r}{\partial \theta_1} = \frac{\partial \sigma(\max(\mathbf{q}_t) - \lambda)}{\partial \max(\mathbf{q}_t)} \cdot \frac{\partial \max(\mathbf{q}_t)}{\partial \mathbf{q}_t} \cdot \frac{\partial \mathbf{q}_t}{\partial \theta_1} \quad (8)$$

Since $\frac{\partial \sigma(x)}{\partial x} = \sigma(x)(1 - \sigma(x))$, plugging it in Eq.(7) we get:

$$\frac{\partial f_r}{\partial \theta_1} = \sigma(\max(\mathbf{q}_t) - \lambda)(1 - \sigma(\max(\mathbf{q}_t) - \lambda)) \cdot \frac{\partial \max(\mathbf{q}_t)}{\partial \mathbf{q}_t} \cdot \beta \frac{\partial Q(s_t, a_t, \theta_1)}{\partial \theta_1}.$$

Now, the gradient of L_r with respect to θ_1 and θ_2 can be computed using the chain rule. The gradient with respect to θ_1 is:

$$\frac{\partial L_r}{\partial \theta_1} = \frac{1}{\mu B} \sum_{t=1}^{\mu B} \left[\frac{\partial f_r}{\partial \theta_1} e_t^2 + f_r \cdot 2e_t \cdot \frac{\partial \alpha(\mathbf{q}_t, \lambda)}{\partial \theta_1} \right].$$

Similarly, for θ_2 , the gradient is:

$$\frac{\partial L_r}{\partial \theta_2} = \frac{1}{\mu B} \sum_{t=1}^{\mu B} \left[\frac{\partial f_r}{\partial \theta_2} e_t^2 + f_r \cdot 2e_t \cdot \frac{\partial \alpha(\mathbf{q}_t, \lambda)}{\partial \theta_2} \right].$$

Thus, we have derived the gradient of the loss function L_r with respect to θ_1 and θ_2 , taking into account the sigmoid approximation of the indicator function.

A.3 The Gradient of L_s

The loss function L_s is:

$$L_s = \frac{1}{(1 - \mu)B} \sum_{t=1}^{(1-\mu)B} [\mathbb{1}(\max(\mathbf{q}_t^s) \geq \lambda, \max(\mathbf{q}_t^w) \geq \lambda) \times \mathcal{H}(\mathbf{q}_t^{w,'}, \mathbf{q}_t^{s,'})].$$

To compute $\partial L_s / \partial \theta_1$, we will apply the chain rule. The loss L_s involves a sum of products, and we need to consider the parts that depend on θ_1 . We adopt the same approach as in Section A.2, using sigmoid function (see Eq.(6)) approximation for the indicator function. Therefore, the overall approximation of the indicator function is:

$$\mathbb{1}(\max(\mathbf{q}_t^s) \geq \lambda, \max(\mathbf{q}_t^w) \geq \lambda) \approx \sigma(\max(\mathbf{q}_t^s) - \lambda) \cdot \sigma(\max(\mathbf{q}_t^w) - \lambda). \quad (9)$$

Similar to that in Appendix.A.2, the approximate derivative of the indicator function $\mathbb{1}(\max(\mathbf{q}_t^s) \geq \lambda, \max(\mathbf{q}_t^w) \geq \lambda)$ (denoted as f_s) with respect to θ_1 is computed based on Eq.(8) and Eq.(9):

$$\begin{aligned} \frac{\partial f_s}{\partial \theta_1} &= \sigma(\max(\mathbf{q}_t^s) - \lambda)(1 - \sigma(\max(\mathbf{q}_t^s) - \lambda)) \cdot \sigma(\max(\mathbf{q}_t^w) - \lambda) \cdot \frac{\partial \max(\mathbf{q}_t^s)}{\partial \theta_1} \\ &\quad + \sigma(\max(\mathbf{q}_t^s) - \lambda) \cdot \sigma(\max(\mathbf{q}_t^w) - \lambda)(1 - \sigma(\max(\mathbf{q}_t^w) - \lambda)) \cdot \frac{\partial \max(\mathbf{q}_t^w)}{\partial \theta_1}. \end{aligned} \quad (10)$$

Then, compute the derivative of the cross-entropy with respect to θ_1 . The cross-entropy between two distributions p and q is given by:

$$\mathcal{H}(p, q) = - \sum_i p_i \log(q_i)$$

where p_i are the true probabilities and q_i are the predicted probabilities. Since $\mathbf{q}_t^{w,'}$ is a one-hot encoded vector, where only one position is 1 and others are 0, the cross-entropy in Eq.(5) is simplified to:

$$\mathcal{H}(p, q) = - \log(q_{i^*})$$

where i^* is the index where $q_1^{w, \prime} = 1$. Therefore, by chain rule the derivative of the cross-entropy with respect to θ_1 is:

$$\begin{aligned} \frac{\partial \mathcal{H}(p, q)}{\partial \theta_1} &= \frac{\partial \mathcal{H}(p, q)}{\partial q_{i^*}} \cdot \frac{\partial q_{i^*}}{\partial \theta_1} \\ &= -\frac{1}{q_{i^*}} \cdot \frac{\partial q_{i^*}}{\partial \theta_1} \end{aligned} \quad (11)$$

The loss L_s involves a sum of products, and now that we have derived the parts that depend on θ_1 in Eq.(10) and Eq.(11), the gradient of the loss function with respect to θ_1 is:

$$\frac{\partial L_s}{\partial \theta_1} = \frac{1}{(1-\mu)B} \sum_{t=1}^{(1-\mu)B} \left[\frac{\partial f_s}{\partial \theta_1} \cdot \mathcal{H}(\mathbf{q}_t^{\mathbf{w}, \prime}, \mathbf{q}_t^{\mathbf{s}, \prime}) - f_s \cdot \frac{1}{q_{i^*}} \cdot \frac{\partial q_{i^*}}{\partial \theta_1} \right].$$

where

$$\begin{aligned} \frac{\partial f_s}{\partial \theta_1} &= \sigma(\max(\mathbf{q}_t^{\mathbf{s}}) - \lambda)(1 - \sigma(\max(\mathbf{q}_t^{\mathbf{s}}) - \lambda)) \cdot \sigma(\max(\mathbf{q}_t^{\mathbf{w}}) - \lambda) \cdot \frac{\partial \max(\mathbf{q}_t^{\mathbf{s}})}{\partial \theta_1} \\ &\quad + \sigma(\max(\mathbf{q}_t^{\mathbf{s}}) - \lambda) \cdot \sigma(\max(\mathbf{q}_t^{\mathbf{w}}) - \lambda)(1 - \sigma(\max(\mathbf{q}_t^{\mathbf{w}}) - \lambda)) \cdot \frac{\partial \max(\mathbf{q}_t^{\mathbf{w}})}{\partial \theta_1}. \end{aligned}$$

Similarly, we can derive the gradient of L_s with respect to θ_2 .

B Supplementary Materials for Experiments

B.1 Hyperparameters Settings

The hyperparameter setup of our experiments in Section 4 consists of the data augmentation parameters, the SSRS framework parameters and other general configurations. As for data augmentation parameters, we adopt consistent settings throughout the experiments in Section 4.1-4.3. Due to different environments, the shapes of states and observations are different, so the parameter n of *double entropy data augmentation* and cutout data augmentation, which is related to the state and observation dimension, are different in Atari and Robotic environments (see Table 2).

Table 2: The explicit value of n of aforementioned transformations in two environments. Note that Double-Ent refers to *double entropy data augmentation*.

VALUE OF n	DOUBLE-ENT	CUTOUT
ATARI	8	16
ROBOTIC	4	3

In Table 3, we present the settings of hyperparameters in SSRS framework, which are based on preliminary hyperparameter tuning results as we mentioned in Section 4. Note that dynamic setting is applied to the consistency coefficient α and the threshold of confidence λ , *i.e.*, the value of these hyperparameters change during the training process, and the value shown in the Table 3 is the final value of the dynamic setting. In detail, the confidence threshold λ grows along with the training iteration. In a training process with N_{iter} iteration in total, λ is as followed at the n_{iter} iteration:

$$\lambda = 0.6 + 0.3 \times \left(1 - e^{-\frac{n_{iter}}{N_{iter}}}\right)$$

Similarly, in a training process with N_{iter} iteration in total, the consistency coefficient α is as followed at the n_{iter} iteration:

$$\alpha = \begin{cases} 0.2 + (0.7 - 0.2) \times \left(\frac{n_{iter}}{N_{iter} \times 0.8}\right), & \text{if } n_{iter} < 0.8 \cdot N_{iter} \\ 0.7, & \text{otherwise} \end{cases}$$

Table 3: The setting of hyperparameters in SSRS framework.

HYPERPARAMETER	DESCRIPTION	VALUE
β	THE QV CONFIDENCE COEFFICIENT	0.5
λ	THE THRESHOLD OF CONFIDENCE	0.9
α	THE CONSISTENCY COEFFICIENT	0.7
p_u	THE UPDATE PROBABILITY	0.01
N_z	THE SIZE OF THE FIXED REWARD SET Z	12
n	PARTITION NUMBER OF DOUBLE ENTROPY AUGMENTATION	8

The network architecture, training parameters, and other hyperparameters used in the experiments for the base DQN, DDPG, PER and ICM algorithms follow the settings provided by the Tianshou RL Library Weng u. a. (2022) and each paper Mnih u. a. (2015); Lillicrap u. a. (2015); Schaul u. a. (2015); Pathak u. a. (2017). The hyperparameter settings of RCP refer to the settings in the code base Bricken (2021) and paper Kumar u. a. (2019). Additionally, the network architecture of the reward estimator is also presented in Table 4.

B.2 List of Data Augmentation Methods

Various types of data augmentation methods are used in the process of *consistency regularization*. Since the transformation *double entropy data augmentation* is thoroughly stated in Section 3.1, we here list all transformation operations for data augmentation strategies involved in our experiment in Table 5 for completeness. The parameter setup of the transformation refers to the Appendix B.1.

Regarding to the heterogeneous SSRS variants which apply two weak and strong data augmentations in *consistency regularization*, the transformation details of the legends in Figures 5 are listed below:

- **SSRS-S:** SSRS-S applies σ random gauss noise as the weak augmentation and *double entropy data augmentation* as strong augmentation.
- **SSRS-M:** SSRS-M applies σ random gauss noise as the weak augmentation and smooth data augmentation as strong augmentation.
- **SSRS-C:** SSRS-C applies σ random gauss noise as the weak augmentation and cutout data augmentation as strong augmentation.

Table 4: Network architecture and hyperparameters

ARCHITECTURE AND HYPERPARAMETERS		VALUE
VALUE NETWORK		- CONV(32-8x8-4) / RELU
		- CONV(64-4x4-2) / RELU
		- CONV(64-3x3-1) / RELU
		- FLATTEN
		- FC(512) / RELU
		- FC(A)
REWARD		- FC(128) / RELU
		- DROPOUT(P=0.2)
		- FC(64) / RELU
		- DROPOUT(P=0.2)
		- FC(32) / RELU
		- DROPOUT(P=0.2)
		- FC(N_z) / RELU
	- SOFTMAX(DIM=-1)	
DQN	DISCOUNT FACTOR γ	0.99
	LEARNING RATE	0.0001
	BATCH SIZE	256
	NUMBER OF PARALLEL ENVIRONMENTS	8
	ESTIMATION STEP	3
	TARGET UPDATE FREQUENCY	500
DDPG	DISCOUNT FACTOR γ	0.99
	ACTOR LEARNING RATE	0.001
	CRITIC LEARNING RATE	0.001
	BATCH SIZE	256
	NUMBER OF PARALLEL ENVIRONMENTS	8
	UPDATE PER STEP	1
	SOFT UPDATE τ	0.005
	EXPLORATION NOISE	0.1
PER	PRIORITY BIAS α	0.6
	IMPORTANCE SAMPLING CORRECTION β	0.4
ICM	ICM LEARNING RATE SCALE	0.2
	REWARD SCALE	0.01
	FORWARD LOSS SCALE	0.2
	INTRINSIC CURIOSITY MOUDULE	HIDDEN SIZE=[512]
RCP	β REWARD WEIGHTING	1
	MAX LOSS WEIGHTING	20
	TD λ	0.95

Table 5: Data augmentation methods in the control group and SSRS variants. Weak augmentation is gauss augmentation by default, and the rest augmentations are used as strong augmentations respectively.

TRANSFORMATION	DESCRIPTION	PARAMETER	RANGE
GAUSS	ADD σ RANDOM GAUSS NOISE TO THE OBSERVATION	σ	<i>default</i> = 0.1
CUTOUT	RANDOMLY ZERO OUT n COLUMNS OF OBSERVATION	n	<i>default</i> = 16
SMOOTH	SMOOTH n CONSECUTIVE OBSERVATIONS	n	<i>default</i> = 3
SCALE	SCALE THE OBSERVATION BY RANDOM SCALE FACTOR λ	λ	(0.8, 1.2)
TRANSLATION	HORIZONTALLY TRANSLATE THE OBSERVATION BY FACTOR λ	λ	(0, 0.1)
FLIP	HORIZONTALLY MIRROR FLIP THE OBSERVATION		